Available online at www.sciencedirect.com
ScienceDirect
Journal of the European Ceramic Society 27 (2007) 3713–3717
www.elsevier.com/locate/jeurceramsoc

Far-infrared and THz spectroscopy of 0.4PMN–0.3PSN–0.3PZN relaxor ferroelectric ceramics

J. Macutkevic [a], S. Kamba [b], J. Banys [a,*], A. Pashkin [b], K. Bormanis [c], A. Sternberg [c]

[a] Faculty of Physics, Vilnius University, Sauletekio 9, 2040 Vilnius, Lithuania
[b] Institute of Physics, ASCR, Na Slovance 2, 18221 Prague 8, Czech Republic
[c] Institute of Solid State Physics, University of Latvia, 8 Kengaraga Str., 1063 Riga, Latvia

Available online 19 March 2007

Abstract

Temperature dependence of the optic phonons in $0.4PbMg_{1/3}Nb_{2/3}O_3$–$0.3PbSc_{1/2}Nb_{1/2}O_3$–$0.3PbZn_{1/3}Nb_{2/3}O_3$ (0.4PMN–0.3PSN–0.3PZN) ceramics were studied by means of FTIR reflection and THz transmission spectroscopy in the temperature range of −253.15 to 226.85 °C. On heating from low temperatures, the A_1 component of the strongly split TO_1 mode softens towards the Burns temperature, but the softening ceases near 126.85 °C which could be a signature of polar cluster percolation temperature. Surprisingly, the TO_2 mode also softens on heating and follows the Cochran law with extrapolated critical temperature close to the melting point.

Keywords: Sintering; Spectroscopy; Ferroelectric properties; Perovskites; Traditional ceramics

1. Introduction

Solution of relaxor ferroelectric enigma is still one of the most challenging problems in the physics of ferroelectrics. Since the discovery of the archetypical relaxor material $PbMg_{1/3}Nb_{2/3}O_3$ (PMN),[1] the origin of its key features – (i) anomalous broad dielectric dispersion at low temperatures, (ii) non-ergodic behavior, and (iii) virtually no symmetry breaking after zero field cooling down to lowest temperatures – has been discussed controversially.[2–5] No breaking of cubic symmetry was observed in PMN at any temperature without bias electric field,[6] however for $PbSc_{1/2}Nb_{1/2}O_3$ (PSN) and $PbZn_{1/3}Nb_{2/3}O_3$ (PZN) a ferroelectric phase transition from cubic to rhombohedral phase was reported near 104.85 °C,[7] and 136.85 °C,[8] respectively. Nevertheless, there are indications from various experiments that the cubic crystal symmetry in relaxors ferroelectrics becomes locally broken already at about 26.85 °C above the temperature of permittivity maximum T_m at the Burns temperature T_B.[9] The nanoregions, in which the cubic structure is broken, are called polar nanoclusters or polar nanoregions. Concerning their symmetry, many authors assume that the nanoregions have the same symmetry as the low-temperature ferroelectric phase, i.e. rhombohedral with polarization along [1 1 1] direction. Nevertheless some authors claim that the nanoclusters have different symmetry with [1 1 0]-type or even [1 0 0]-type polarization.[10–12]

Ternary solid solutions of PSN–PZN–PMN relaxor ferroelectrics have been first synthesized and investigated by Dambekalne et al.[13] The system was very well soluble and the dielectric data showed high values of permittivity (7000–30,000) with diffused peak typical for relaxor ferroelectric. Results of broadband dielectric spectroscopy of 0.2PMN–0.4PSN–0.4PZN and 0.4PSN–0.3PMN–0.3PZN ceramics were published by some of us.[14–16]

The aim of the present work is to investigate infrared (IR) and THz spectra of 0.4PMN–0.3PSN–0.3PZN relaxor ceramics with emphasis on discussion of activities and temperature dependences of optic phonons in IR spectra.

2. Experimental

The ternary 0.4PMN–0.3PSN–0.3PZN solid solution was synthesized by solid-state reactions from high grade oxides PbO_3, Nb_2O_5, MgO, ZnO, Sc_2O_3. Detailed forming and sintering conditions are presented in Ref. 13.

Measurements at THz frequencies from 3 to 30 cm^{-1} (90–900 GHz) were performed in the transmission mode using a time-domain THz spectrometer based on an amplified femtosecond laser system. Two ZnTe crystal plates were used to generate

* Corresponding author.
E-mail address: juras.banys@ff.vu.lt (J. Banys).

0955-2219/$ – see front matter
doi:10.1016/j.jeurceramsoc.2007.02.023

(by optic rectification) and detect (by electro-optic sampling) the THz pulses. A polished plane-parallel 40 μm-thick plates with a diameter of 6 mm were investigated. An Optistat CF cryostat with thin mylar windows was used for measurements down to −193.15 °C. For sample heating up to 549.85 °C, we used an adapted commercial high-temperature cell (SPECAC P/N 5850) with 1 mm-thick sapphire windows. IR reflectivity spectra were obtained using a FTIR spectrometer Bruker IFS 113v in the frequency range of 20–3300 cm^{-1} (0.6–100 THz) above room temperature, at lower temperature the reduced spectral range up to 650 cm^{-1} was investigated because this is the transparency region of polyethylene windows in the cryostat (Oxford Inst.). Pyroelectric deuterated triglicine sulfate detectors were used for the room and higher temperature measurements, while more sensitive helium cooled (−271.65 °C) Si bolometer was used for low-temperature measurements. Home-made furnace was used for high-temperature experiments up to 249.85 °C. Polished disk-shaped samples with a diameter of 6 mm and thickness of about 2 mm were investigated.

3. Results and discussion

IR and THz reflectivity spectra of 0.4PMN–0.3PSN–0.3PZN ceramics taken at various temperatures are shown in Fig. 1. Reflectivity spectra below 30 cm^{-1} were calculated from THz transmission spectra. The spectral range above 800 cm^{-1} is not shown because the reflectivity is almost flat at higher frequencies approaching the value given by the high-frequency permittivity ε_∞. IR reflectivity and THz dielectric spectra were fitted simultaneously using a generalized-oscillator model of the factorized form of the complex permittivity:

$$\varepsilon*(\omega)=\varepsilon'(\omega)-\mathrm{i}\varepsilon''(\omega)=\varepsilon_\infty\prod_j\frac{\omega_{\mathrm{LO}_j}^2-\omega^2+\mathrm{i}\omega\gamma_{\mathrm{LO}_j}}{\omega_{\mathrm{TO}_j}^2-\omega^2+\mathrm{i}\omega\gamma_{\mathrm{TO}_j}}, \quad (1)$$

where ω_{TO_j} and ω_{LO_j} mark the transverse and longitudinal frequency of the jth mode, respectively, and γ_{TO_j} and γ_{LO_j} denote their corresponding damping constants. $\varepsilon^*(\omega)$ is related to reflectivity $R(\omega)$ by

$$R(\omega)=\left|\frac{\sqrt{\varepsilon*(\omega)}-1}{\sqrt{\varepsilon*(\omega)}+1}\right|. \quad (2)$$

The high-frequency permittivity ε_∞ resulting from electronic absorption processes was obtained from the frequency-independent room temperature reflectivity above the phonon frequencies. The obtained value of ε_∞ is equal to 5.87—the same as in pure PMN.[17] Temperature dependence of ε_∞ is usually very small and was neglected in our fits.

Eight polar phonons were resolved in the fits of reflectivity below −123.15 °C, seven modes at higher temperatures. This is inconsistent with factor-group analysis for cubic and rhombohedral symmetry, where only 3 and 16 IR active modes, respectively, are allowed in the IR spectra. If we assume that the ceramics have macroscopically cubic symmetry with the polar nanoregions of rhombohedral symmetry, the IR probe is enough sensitive to observe the polar modes from rhombohedral structure. Nevertheless, we do not see all the modes allowed in the rhombohedral phase because some of them could be weak and/or overlapped with others due to their finite dampings.

Real and imaginary parts of $\varepsilon^*(\omega)$ obtained from the fits of IR reflectivity and THz dielectric spectra are shown in Fig. 2. The low-frequency part of the IR and THz spectrum was fitted with an overdamped oscillator. Of course, this model cannot completely fit the static permittivity due to presence of microwave (MW) relaxation below our frequency range, but it can at least roughly describe the high-frequency wing of MW relaxation seen in the THz spectra. Dielectric contribution of the overdamped oscillator increases with temperature, because the relaxation frequency of the microwave relaxation hardens and approaches to THz range.

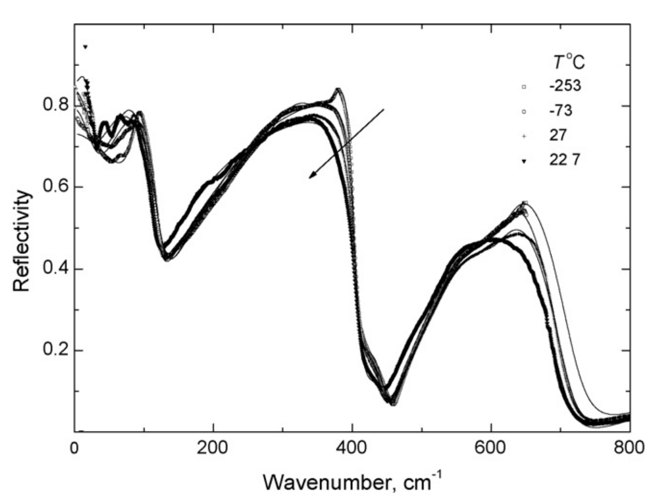

Fig. 1. IR and THz reflectivity spectra of 0.4PMN–0.3PSN–0.3PZN ceramics at various temperatures. Solid lines are results of the fits.

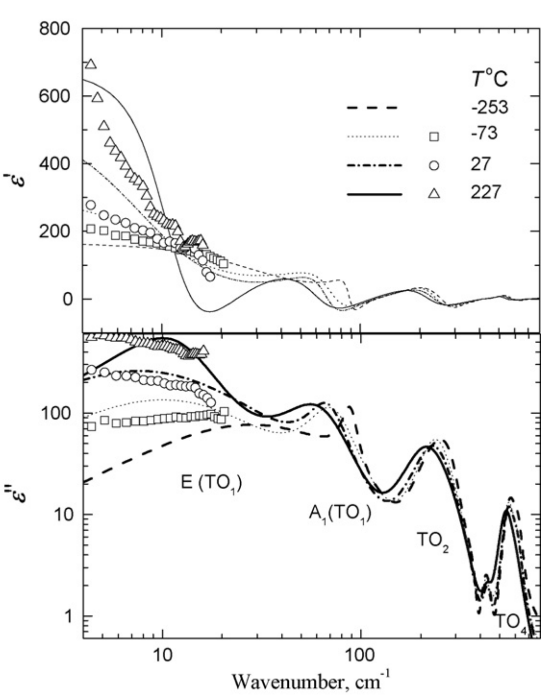

Fig. 2. Complex dielectric permittivity obtained from the fit of IR and THz spectra of 0.4PMN–0.3PSN–0.3PZN ceramics.

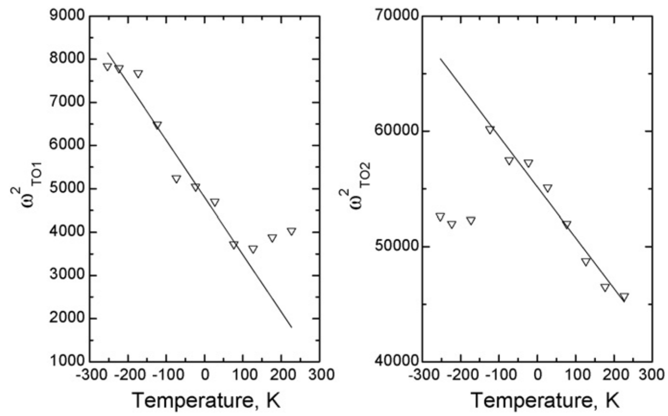

Fig. 3. Cochran fit to TO_1 and TO_2 modes in 0.4PMN–0.3PSN–0.3PZN.

Interesting phonon anomalies were observed. Most of phonon frequencies exhibit softening on heating, the most remarkable softening is seen for the lowest frequency TO_1 phonon (see Fig. 3a). Similar soft TO_1 mode was observed in PMN and PST.[18–20] This mode was explained as a ferroelectric soft mode in polar clusters,[18] which softens close to the Burns temperature. The soft mode frequency follows the Cochran law:

$$\omega_{SM}^2 = A(T_{cr} - T), \tag{3}$$

where constant $A = 13.22\,cm^2/K$ and $T_{cr} = -273.15\,°C$ means the critical softening temperature. It is really difficult to speculate that T_{cr} temperature corresponds to the Burns temperature, because the experimental TO_1 frequency starts to increase already above 126.85 °C. We would like to stress that non-complete softening of TO_1 mode was observed in all previously studied perovskite relaxors,[21,16] as well as in slightly doped incipient ferroelectric $KaTa_{1-x}Nb_xO_3$.[22] For example, in pure PMN[18,19] the soft mode followed the Cochran law up to 176.85 °C and it leveled off at higher temperatures. In $KaTa_{1-x}Nb_xO_3$ ($x = 0.012$) the soft mode reaches minimum frequency at −253.15 °C and again hardens below this temperature, although no structural phase transition occurs at this temperature.[22] This effect was correlated with the appearance of the polar clusters[22,23] and understood taking into account the lattice anharmonicity induced by polar clusters.[24]

Recently, Toulouse at al.[25] investigated PZN relaxor by means of Raman scattering and reported about a new critical temperature $T_l \cong 196.85\,°C$, which he called "temperature of local phase transition" or temperature of creation of polar clusters. According to Toulouse at al.[25] the Burns temperature near 326.85 °C is just the temperature, below which the anharmonic vibration of Pb atoms becomes slower than the frequency of F_{1u} soft mode. We speculate that the T_l temperature corresponds to temperature, below which the polar clusters are percolated. The effective soft mode cannot completely soften in the system of non-percolated clusters[26] due to rise of effective soft phonon frequency in the composite of polar clusters with non-polar matrix. Therefore, the leveling off (or even increase) of the soft mode frequency is seen above $T_l \approx 126.85\,°C$.

Surprisingly, the TO_2 polar mode frequency also softens on heating and follows the Cochran law (see Fig. 3b). The T_{cr} of TO_2 mode is equal to 1252.85 °C and $A = 44.01\,cm^2/K$. This mode is so called Slater mode describing predominantly vibration of B atoms against oxygen octahedral.[21] The B sites exhibit large chemical disorder (four various atoms of different valency!) and temperature T_{cr} of TO_2 modes can correspond to temperature, where the B site atoms could migrate, because its value is close to a melting point. The list of polar mode parameters (at −253.15 °C) in investigated 0.4PMN–0.3PSN–0.3PZN ceramics is summarized in Table 1. The parameters of investigated ceramics are very similar and comparison with pure PMN[17–19] as well as with PST[20] shows that the spectra of all perovskite relaxors have the same features: original three F_{1u} cubic perovskite modes are split due to lower symmetry in polar nanoclusters. The most remarkable splitting is seen in the soft mode at −253.15 °C. Its A_1 component has frequency near $90\,cm^{-1}$, while the E component is heavily damped and has frequency near $20\,cm^{-1}$. The value of mode splitting is not dependent whether the sample exhibits structural phase transition (like PST)[20] or not (like PMN),[19] because the FIR spectroscopy is sensitive just on local order and the FIR wave does not feel any difference between distorted structure in polar nanoclusters and ferroelectric domains.

Detail assignment of polar modes in perovskite relaxors was recently thoroughly discussed[21]: the modes below $100\,cm^{-1}$ are so called Last modes expressing predominantly the vibration of rigid BO_6 octahedra against Pb atoms. Two modes between 200 and $300\,cm^{-1}$ are E and A_1 components of the Slater modes (vibration of B atoms against O_6 octahedra) and the modes above $500\,cm^{-1}$ are Axe modes[21] (bending of the O_6 octahedra). The mode near $380\,cm^{-1}$ is activated in the spectra only due to the local order in the B sites and express the mutual B atoms vibra-

Table 1
Polar mode parameters of the 0.4PMN–0.3PSN–0.3PZN ceramics obtained from the fit to the −253.15 °C reflectivity by means of Eqs. (1) and (2)

ω_{TO}	γ_{TO}	ω_{LO}	γ_{LO}	Assignment
29.4	21.2	39.5	59.5	E component of TO_1
88.2	19.2	118.7	32.4	A_1 component of TO_1
241.4	157.2	406.8	14.7	E component of TO_2
292	111.4	289.3	440.1	A_1 component of TO_2
379.4	80.1	354.1	84.5	From Bril. zone boundary
434.3	55.7	444.4	18.4	Resonance between E LO_2 and A_1 LO_2—see Ref. 27
568.2	89.2	703.8	60.3	E component of TO_4
626.4	66.7	610.2	107.4	A_1 component of TO_4

All parameters are in cm^{-1}, $\varepsilon_\infty = 5.87$.

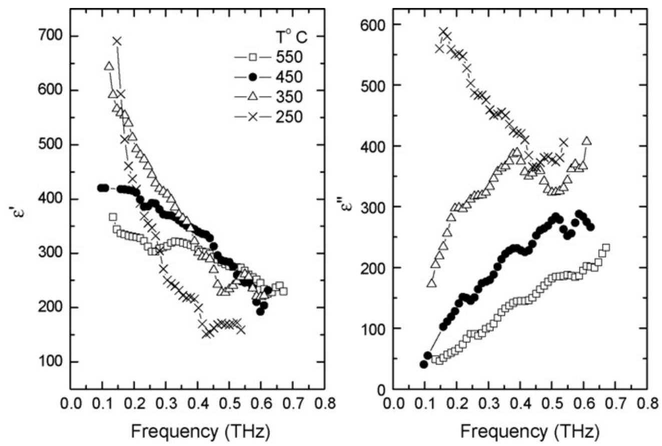

Fig. 4. Complex THz dielectric spectra of 0.4PMN–0.3PSN–0.3PZN ceramics at various temperatures.

tions with wavevector from Brillouin zone boundary. Hlinka et al.[27] recently used the effective medium approximation for the evaluation of room temperature IR reflectivity spectra of PMN and showed that this approach can be used for determination of anisotropic dielectric functions (i.e. also of parameters of modes of different symmetries) in polar clusters. It follows from this analysis that the mode near 430 cm^{-1} (seen also in our spectra), is not a real polar phonon but just apparent mode which appears in the IR spectra as consequence of resonances between two longitudinal modes.[27]

Fig. 2 shows a broad maximum of $\varepsilon''(\omega)$ near 30 cm^{-1} (at −253.15 °C) which corresponds to the E component of the soft mode. This mode softens to about 20 cm^{-1} at −73.15 °C, however at higher temperatures is this mode overlapped by the dielectric relaxation which approaches this frequency range from microwave region and which is seen as a peak near 7 cm^{-1}. Fig. 4 shows the THz dielectric spectra at high temperatures up to 599.85 °C. One can see that the relaxation hardens on heating, passes through our frequency range but remains in the spectra also at 599.85 °C. The evidence for it is the decrease of ε' with frequency seen in Fig. 4 at all temperatures. In the case of no relaxation in the spectra would be $\varepsilon'(\omega)$ frequency-independent and its value would be determined just by phonon contributions. Because the relaxation comes from dynamics (predominantly from flipping) of polar clusters, our spectra gives evidence, that the clusters exist in 0.4PMN–0.3PSN–0.3PZN at least up to 599.85 °C and that the Burns temperature is higher.

4. Conclusion

We would like to conclude that our far infrared spectra of 0.4PMN–0.3PSN–0.3PZN solid solution give evidence about locally broken cubic symmetry in the sample due to polar clusters of lower symmetry. Ferroelectric soft mode in polar clusters was observed, but its softening ceases above 126.85 °C. This effect was explained by the polar cluster percolation below 126.85 °C. Softening of TO_2 polar mode was also observed on heating. This effect was never observed in other relaxor ferroelectrics. TO_2 phonon frequency follows the Cochran law with extrapolated critical temperature near melting point. THz dielectric spectra revealed that the microwave relaxation hardens on heating and approaches THz frequency range above 226.85 °C. Its strength gradually decreases on heating, but remains in the spectra up to 549.85 °C. It means that the polar clusters do not disappear suddenly, but remain in the structure up to our highest temperature.

Acknowledgements

This work was supported by Lithuanian States and Studies Foundation and by the Grant Agency of the Czech Republic (projects nos. 202/06/0403 and 202/04/0993).

References

1. Smolenskii, G. A. and Agranovskaya, A. I., Dielectric polarization and losses of some complex compounds. *Soviet Phys., Tech. Phys.*, 1958, **3**, 1380.
2. Kleemann, W., Random-field induced antiferromagnetic, ferroelectric and structural domain states. *Int. J. Mod. Phys. B*, 1993, **7**, 2469.
3. Vugmeister, B. E. and Rabitz, H., Dynamics of interacting clusters and dielectric response in relaxor ferroelectrics. *Phys. Rev. B*, 1998, **57**, 7581.
4. Vugmeister, B. E., Polarization dynamics and formation of polar nanoregions in relaxor ferroelectrics. *Phys. Rev. B*, 2006, **73**, 174117.
5. Blinc, R. and Pirc, S., Spherical random-bond–random-field model of relaxor ferroelectrics. *Phys. Rev. B*, 1999, **60**, 13470.
6. de Mathan, N., Husson, E., Calvarin, G., Gavari, J. R., Hewat, A. W. and Morell, A., A structural model for the relaxor $PbMg_{1/3}Nb_{2/3}O_3$ at 5 K. *J. Phys.: Condens. Matter*, 1991, **3**, 8159–8171.
7. Perrin, C., Menguy, N., Suard, E., Muller, Ch., Caranoni, C. and Stepanov, A., Neutron diffraction study of the relaxor-ferroelectric phase transition in disordered $PbSc_{1/2}Nb_{1/2}O_3$. *J. Phys.: Condens. Matter*, 2000, **12**, 7523–7539.
8. Kisi, E. H. and Forester, J. S., Crystal structure of the relaxor ferroelectric PZN: demise of the 'X phase'. *J. Phys.: Condens. Matter*, 2005, **17**, L381–L384.
9. Burns, G. and Dacol, F. H., Crystalline ferroelectrics with glassy polarization behavior. *Phys. Rev. B*, 1983, **28**, 2527.
10. Guangyong, Xu., Zhong, Z., Bing, Y., Ye, Z.-G. and Shirane, G., Electric-field-induced redistribution of polar nano-regions in a relaxor ferroelectric. *Nat. Mater.*, 2006, **5**, 134.
11. Jeong, I. K., Darling, T. W., Lee, J. K., Proffen, T., Heffner, R. H., Park, J. S. *et al.*, Direct observation of the formation of polar nanoregions in PMN using neutron pair distribution function analysis. *Phys. Rev. Lett.*, 2003, **91**, 247601.
12. Dkhil, B., Kiat, J. M., Calvarin, G., Baldinozzi, G., Vakhrushev, S. B. and Suard, E., Local and long range polar order in the relaxor-ferroelectric compounds $PbMg_{1/3}Nb_{2/3}O_3$ and $PbMg_{0.3}Nb_{0.6}Ti_{0.1}O_3$. *Phys. Rev. B*, 2002, **65**, 024104.
13. Dambekalne, M., Bormanis, K., Sternberg, A. and Brante, I., Relaxor ferroelectric $PbSc_{1/2}Nb_{1/2}O_3$–$PbZn_{1/3}Nb_{2/3}O_3$–$PbMg_{1/3}Nb_{2/3}O_3$ ceramics. *Ferroelectrics*, 2000, **240**, 221–228.
14. Macutkevic, J., Lapinskas, S., Grigas, J., Brilingas, A., Banys, J., Grigalaitis, R. *et al.*, Distribution of the relaxation times of the new relaxor 0.4PSN–0.3PMN–0.3PZN ceramics. *J. Eur. Ceram. Soc.*, 2005, **25**, 2515–2519.
15. Banys, J., Macutkevic, J., Brilingas, A., Grigas, J., Bormanis, K. and Sternberg, A., Radio and microwave spectroscopy of 0.2PMN–0.4PSN–0.4PZN ceramics. *Ferroelectrics*, 2005, **318**, 141–146.
16. Macutkevic, J., Kamba, S., Banys, J., Brilingas, A., Pashkin, A., Petzelt, J. *et al.*, Infrared and broad-band dielectric spectroscopy of PZN–PMN–PSN

relaxor ferroelectrics: Origin of two-component relaxation. *Phys. Rev. B.*, 2006, **74**, 104106.
17. Prosandeev, S. A., Cockayne, E., Burton, B. P., Kamba, S., Petzelt, J., Yuzyuk, Yu. *et al.*, Lattice dynamics in $PbMg_{1/3}Nb_{2/3}O_3$. *Phys. Rev. B*, 2004, **70**, 134110.
18. Bovtun, V., Kamba, S., Pashkin, A., Savinov, M., Samoukhina, P. and Petzelt, J., Central peak components and polar soft mode in relaxor $PbMg_{1/3}Nb_{2/3}O_3$ crystals. *Ferroelectrics*, 2004, **298**, 23–30.
19. Kamba, S., Kempa, M., Bovtun, V., Petzelt, J., Brinkman, K. and Setter, N., Soft and central mode behaviour in $PbMg_{1/3}Nb_{2/3}O_3$ relaxor ferroelectric. *J. Phys.: Condens. Matter*, 2005, **17**, 3965–3974.
20. Kamba, S., Berta, M., Kempa, M., Petzelt, J., Brinkman, K. and Setter, N., Far-infrared soft mode behavior in $PbSc_{1/2}Ta_{1/2}O_3$ thin films. *J. Appl. Phys.*, 2005, **98**, 074103.
21. Hlinka, J., Petzelt, J., Kamba, S., Noujni, D. and Ostapchuk, T., Infrared dielectric response of relaxor ferroelectrics. *Phase Trans.*, 2006, **79**, 41–78.
22. Chou, H., Shapiro, S. M., Lyons, K. B., Kjems, J. and Rytz, D., Soft-mode behaviour and the dipolar glass transition in $KTa_{1-x}Nb_xO_3$. *Phys. Rev. B*, 1990, **41**, 7231.
23. DiAntonio, P., Vugmeister, B. E., Toulouse, J. and Boatner, L. A., Polar fluctuations and first-order Raman scattering in highly polarizable $KTaO_3$ crystals with off-center Li and Nb ions. *Phys. Rev. B*, 1993, **47**, 5629.
24. Vugmeister, B. E., Dipole admixture induced lattice anharmonicity near ferroelectric phase transition. *Sov. Phys. Solid State*, 1985, **27**, 716.
25. Toulouse, J., Jiang, F., Svitelskiy, O., Chen, W. and Ye, Z. G., Temperature evolution of the relaxors dynamics in $PbZn_{1/3}Nb_{2/3}O_3$: a critical Raman analysis. *Phys. Rev.*, 2005, **72**, 184106.
26. Rychetsky, I. and Petzelt, J., Dielectric spectra of grainy high-permittivity materials. *Ferroelectrics*, 2004, **303**, 137–140.
27. Hlinka, J., Ostapchuk, T., Nouni, D., Kamba, S. and Petzelt, J., Anisotropic dielectric function in polar nanoregions of relaxor ferroelectrics. *Phys. Rev. Lett.*, 2006, **96**, 027601.